Thermophoretic Transport and Deposition of Particles in Vertical Tube Flow with Variable Wall Temperature and Thermal Radiation

Sung Ho Park*, Won Jin Kim and Sang Soo Kim*****

(*Received November 22, 1997*)

A particulate two phase flow with variable wall temperature has been studied for examining the deposition of particles in the thermal radiation and mixed convection flow associated with the manufacture of optical fiber preforms. The two-dimensional governing equations of continuity, momentum and energy have been solved numerically including the effects of thermal radiation and buoyancy(upward or downward flow) in the vertical tube flow. A particle trajectory model has been adopted to predict the particle transport, and P-1 approximation has been used to evaluate the radiation heat transfer. In the upward flow case, a high deposition efficiency is obtained and the deposition zone of the downward flow is broader than that of the upward flow. Thermal radiation makes the deposition zone broader and the deposition efficiency smaller.

Key Words: Thermophoresis, Thermal Radiation, Absorption Coefficient, Particle Trajectory, Deposition Efficiency

Nomenclature

C_p : Specific heat
D_p : Particle diameter
g : Gravitational acceleration
I_b : Blackbody radiation intensity
I_0 : Zeroth-order moment of intensity
K : Thermophoretic coefficient equation (2)
Kn : Knudsen number, $2\lambda/D_p$
k : Conductivity
l/min : Liter per minute
q_p^r : Radiative heat flux for particle phase
R : Tube radius
r : Radial coordinate
t : Time
T : Temperature
U_{av} : Average gas velocity over the cross section of tube
V : Velocity vector defined by equation (9)
v_T : Thermophoretic velocity vector, equation (1)
v_{Tr} : Thermophoretic velocity of radial direction
x : Axial coordinate.

Greek symbols

β : Extinction coefficient, $k_0+\sigma_0$
ε : Surface emissivity
η : Cumulative deposition efficiency
k_0 : Absorption coefficient
λ : Mean free path of carrier gas
μ : Dynamic viscosity of gas
ν : Kinematic viscosity of gas
ρ_g : Gas density
ρ_p : Aapparent particle density
σ_{pm} : Material density of single particle
σ : Stefan-Boltzmann constant
τ_f : Flow characteristic time
τ_{mon} : Momentum relaxation time
τ_0 : Optical thickness
τ_{th} : Thermal relaxation time, $\rho_{pm}C_{pp}D_p^2/12k_g$

* Dept. of Mechanical Design, Kyungil University
** Dept. of Automotive Engineering, Keimyung University
*** Dept. of Mechanical Engineering, KAIST

Subscript

g : Gas
in : Tube inlet
p : Particle
w : Wall surface

1. Introduction

The thermophoresis is known as a phenomenon in which small particles suspended in a gas medium migrate from hot zone to cold zone of the gas. This thermophoretic force is a result of greater momentum transfer from the gas molecules on the hot side of the particles compared to the cold side. The thermophoretic deposition of fine particles is of practical importance in various industrial applications such as glass particle deposition onto a quartz surface used in the modified chemical vapor deposition (MCVD) process for optical fiber fabrication, semiconductor devices and corrosion/fouling/erosion of turbine blades or heat transfer surfaces (Moore and Crane, 1973). Especially, in the MCVD process, particulate gas stream (SiO_2 carried in O_2) is directed through a rotating silica substrate tube that is heated by a hydrogen-oxygen torch traversing cyclically along the tube axis. The particles generated are small enough to be driven thermophoretically and deposited on the inner surface of the tube wall in the downstream of the torch. Situations often arise in which the mixed convection has rather significant influences on the heat transfer of a gas particulate flow in many engineering systems and natural environments. Since the thermophoresis is strongly dependent upon the temperature gradient as mentioned in the earlier studies (Nagel *et al.*, 1982 and Yoa *et al.*, 1991), the radiative effect on the thermophoresis can be significant when absorbing and emitting particles in a high temperature gas-particulate systems. Subsequent studies have focused on understanding the fundamental physics and chemistry of the process, and improving the efficiency of this method of preform fabrication. The thermophoresis is the dominant transport mechanism responsible for the deposition of particles onto the inner wall of the containing tube during the MCVD process as shown experimentally by Simpkins *et al.* (1979) and theoretically by Walker *et al.* (1980). The thermophoretic transport of fly-ash, soot, TiO_2 or MgO particles has been reported experimentally (Rosner and Kim, 1984; Kim and Kim, 1991, 1992; Cho and Choi, 1994). Cho and Choi (1995) experimentally showed that comparison of the measurements of the wall temperature, the particle deposition efficiency, and the tapered entry length is in good agreement with calculations. Upon the basis of this understanding, modification and scale-up of the process have been accomplished to improve both cost effectiveness and manufacturability. In an optical fiber fabrication process, uniform particle deposition along the circumferential direction is important. However, in the horizontal rotating tube, buoyancy leads to asymmetry of temperature, which results in non-uniform particle deposition in the circumferential direction. Rotation of the tube reduces heterogeneous deposition, and by more than 60 rpm (revolution per minute), homogeneous deposition can be achieved to a certain degree. In case of vertical tube with the ring torch, the homogeneous particle deposition of circumferential direction can be expected because of axisymmetric flow and temperature distribution (Choi, 1992; Lin *et al.*, 1992). Morse *et al.* (1985) have considered absorbing, nonemitting particles with low enclosure temperature when the particle is produced by laser heating in the MCVD process. Jia *et al.* (1992) studied radiation and thermophoresis interaction in thermally developing laminar flow through a constant-wal l-temperature parallel-plate channel. Thermophoretic transport and deposition may result in a significant error if the radiation effect for the gas or the particulate phase is omitted, as Goren (1977) pointed out. Park and Kim (1993) studied the effects of particle mass fraction and thermal radiation with isotropic scattering on the forced convection thermophoretic characteristics with uniform wall temperature. In this work, it has been extended to the thermophoretic particle transport and deposition in the vertical tube flow with variable wall temperature and mixed convection and radiation.

2. Analysis

The velocity acquired by small particles relative to the gas velocity (known as thermophoretic velocity) is related to the temperature gradient in the flow field by

$$V_T = -K\nu\nabla \ln T \tag{1}$$

The thermophoretic coefficient K depends mainly on the Knudsen number. The semiempirical formula proposed by Talbot *et al.* (1980) can be used for a wide range of Knudsen numbers.

$$K = 2C_s \frac{(k_g/k_p + C_t Kn)(1 + Kn(1.2 + 0.4\exp(-0.88/Kn)))}{(1+3C_m Kn)(1+2k_g/k_p + 2C_t Kn)} \tag{2}$$

$$Kn = 2\lambda/D_p$$

Here, C_s, C_m and C_t are equal to 1.149, 1.23 and 2.16, respectively (Talbot *et al.*, 1980).

Carrier gas (O_2) is fed into a stationary vertical tube of radius R in fully developed laminar flow. Particles exchange energy with gas in their immediate vicinity, and thus there is negligible temperature slip between gas and particles, because the particle thermal relaxation time is very small compared to the flow characteristic time (τ_{th} is order of 10^{-5}). A dilute gas-particle flow can be assumed owing to the low particle volume fraction, and one-way coupling can be applied to the gas and particle momentum equation because of low particle mass fraction. Carrier gas is assumed to be gray absorbing and emitting without scattering. Particle coagulation associated with Brownian motion leads to a reduction in total number density and increase in the average size, and it is a function of particle number density, particle size and particle residence time. The coagulation time is defined as the time required for the particle field to reduce its number density by 10 percent (Fuch, 1964). It should be mentioned that the particles smaller than about $10^{-2}(\mu m)$ in diameter suspended in a gas exhibit Brownian motion that is sufficiently intense to affect the particle deposition rate. However, for particles with a size of $0.1(\mu m)$ the particle Brownian diffusion coefficient is order of 10^{-5}cm^2/s (Park and Kim, 1993), and thus particle coagulation is negligible. With these assumptions the governing equations of each phase are as follows and the present physical and coordinate system is depicted in Fig. 1.

gas phase (continuous phase)

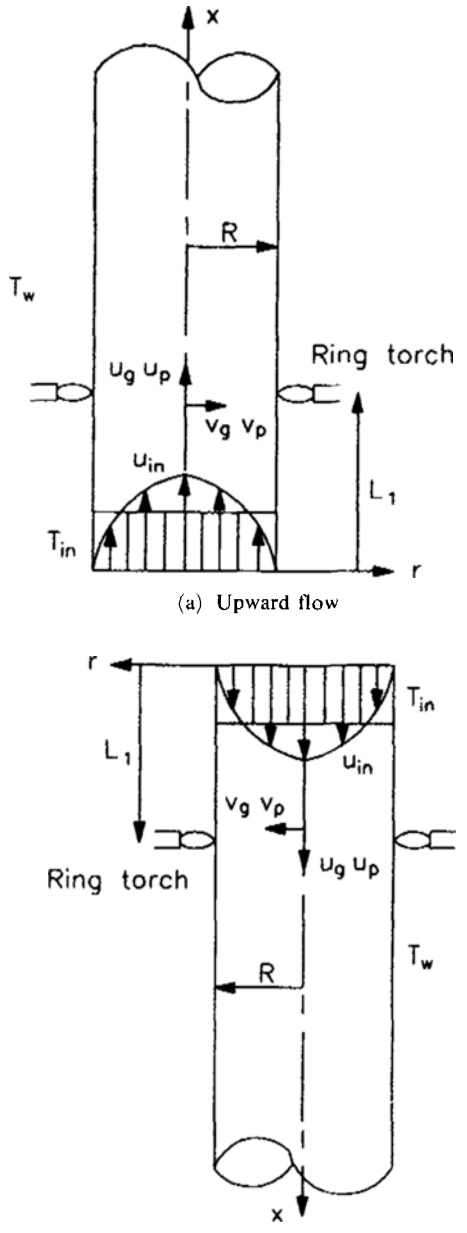

Fig. 1 Schematics of the upward flow (a) and downward flow (b) in the externally heated tube with ring torch

$$\nabla \cdot \rho_g V_g = 0 \tag{3}$$

$$\rho_g V_g \cdot \nabla V_g = \nabla \sigma_g + \rho_p \frac{V_p - V_g}{\tau_{mon}} + \rho_p \frac{K}{\tau_{mon}} \nabla \ln T_g - \rho_g g \tag{4}$$

$$\rho_g C_{pg} V_g \cdot \nabla T_g = \nabla k_g \nabla T_g + \rho_p C_{pp} \frac{T_p - T_g}{\tau_{th}} - \nabla \cdot q_g^r \tag{5}$$

The viscous dissipation and pressure work term in the energy equation are assumed to be negligible. In the gas phase, gas density ρ_g is obtained from the ideal gas law.

particulate phase (dispersed phase)

$$\frac{dV_p(t)}{dt} = \frac{V_g - V_p}{\tau_{mon}} - \frac{K}{\tau_{mon}} \nu \nabla \ln T + g \tag{6}$$

$$\rho_p C_{pp} V_p \cdot \nabla T_g = -\rho_g C_{pp} \frac{T_g - T_p}{\tau_{th}} - \nabla \cdot q_p^r \tag{7}$$

There is negligible temperature slip between gas and particles because the particle thermal relaxation time τ_{th} is very small compared to the flow characteristic time τ_f. To make single energy balance equation, we introduce the mixture energy equation by adding the energy equation of gas and particulate phase. In case of low particle mass fraction, mixture velocity is almost the same as carrier gas velocity in the mixture energy balance equation (Yoa *et al.*, 1991; Park and Kim, 1993).

$$\rho_p C_{pg} V_g \cdot \nabla T_g = \nabla \cdot k_g \nabla T_g - \nabla \cdot q^r \tag{8}$$

The divergence of the net radiative heat flux $\nabla \cdot q^r$ characterizes the net radiative energy emitted or absorbed by the matter per unit time and per unit volume over all frequencies, and can be modelled by the spherical harmonic (P-N) approximation.

$$\rho_p C_{pg} V_g \cdot \nabla T_g = \nabla \cdot k_g \nabla T_g - \kappa_o 4 \sigma T_g^4 \tag{9}$$

The last term in the right hand side of the above equation represents the contribution of thermal radiation, which has been modelled with P-1 approximation. Previous studies indicate that P-1 approximation is more accurate in the optically thick rather than in the optically thin limit (Menguc and Viskanta, 1986). However, P-1 approximation may predict qualitatively, at least, the effect of radiative heat transfer on the thermophoretic particle transport characteristics (Yoa *et al.*, 1991). The radiative transfer equation in terms of P-1 approximation and Marshak's boundary conditions have been showed by Higengi and Bayazitoglu (1980) and Menguc and Viskanta (1986).

$$\frac{1}{\kappa_o}\left[\frac{\partial^2 I_o}{\partial \chi^2} + \frac{1}{r}\frac{\partial}{\partial r}\left(r \frac{\partial I_o}{\partial r}\right)\right] = 3\kappa_o (I_o - 4 I_b \Pi) \tag{10}$$

Boundary conditions:

$$I_o \pm \frac{2}{3}(1 + 2\lambda_w)\left(\frac{\partial I_o}{\partial z}\right)_w = 4 I_{bw} \pi,$$

$$\lambda_w = \frac{1 - \varepsilon_w}{\varepsilon_w} \text{ and } z = x, r \tag{11}$$

$$\left(\frac{\partial I_o}{\partial r}\right)_{r=0} \tag{12}$$

The temperature of the outlet opening section is not known but it is assumed to be thermally fully developed. Thus the temperature near exit is almost same as that of the outlet section. The openings of inlet and outlet are nonreflecting, thereupon, the assumption of a pseudo black wall is applied for the radiation boundary conditions in equation (11). At the tube center, the symmetric condition of temperature suggests that zero moment intensity I_o will not change, as given in equation (12).

Boundary conditions are as follows:

$x = 0$; $u_g = 2 V_{av}(1 - r^2)$, $v_g = 0$, $T = T_i$

$x = L_{max}$; $\frac{\partial u_g}{\partial x} = \frac{\partial v_g}{\partial x} = 0$, $\frac{\partial^2 T}{\partial x^2} = 0$

$r = 0$; $\frac{\partial u_g}{\partial r} = 0$, $v_g = 0$, $\frac{\partial T}{\partial r} = 0$

$r = R$; $u_g = v_g = 0$

$T = T_i + (T_{max} - T_i)\, x / L_1$ for $0 \le x < L_1$

$T = T_i - (T_{max} - T_i)\,(x - L_1)/(L_2 - L_1)$ for $L_1 \le x < L_2$

Table 1 Wall temperature parameters.

Flow rate of carrier gas (Q)	
1 l/min	Re=4.3
3	12.8
L_1 and L_2	20 and 22 cm
T_{in}	1073 K
T_{max}	1973 K
T_{min}	453 K

$T = T_{min}$ for $x \geq L_2$

The temperature profile at the tube wall is a function of axial distance (Walker *et al.*, 1980; Morse *et al.*, 1985). T_i is the inlet temperature at $x=0$, and T_{max} is the maximum temperature just near the oxy-hydrogen torch. For downstream of the torch ($x \geq L_2$), it is assumed that the wall temperature is a constant and equal to T_{min}.

Dilute gas-particle flow and one-way coupling can be applied to the gas and particulate flow field because the particle volume fraction and mass fraction are assumed to be low. However, buoyancy force modifies the hydrodynamic and thermal fields of gas phase, and hence the thermophoretic particle transport may be altered by the combined forced and free convection flows. Nonuniform grids (61×61) have been used in both axial and radial directions. SIMPLER algorithm and the power law differencing scheme have been applied in this work (Patankar, 1980). Since it is assumed that a particle sticks once it reaches the wall (no rebound), a particle is considered to be deposited if it comes within a distance of particle radius to the tube wall. The particle deposition efficiency may be defined as the ratio of the total numbers of deposited particles at the certain axial location to the total number of particles which enter the tube.

3. Results and Discussion

The thermophoretic transport and deposition have been investigated including the effects of the mixed convection and thermal radiation in the vertical tube externally heated with a ring torch (Fig. 1). The present numerical method has been verified by performing calculations for the mixed convection with the constant wall temperature and comparing with Zeldin and Schmidt's results (1972). The cumulative deposition efficiency predicted from the present study has been compared to be in good agreement with that of Walker *et al.* (1979).

The evolutions of the axial velocity profile with or without thermal radiation are shown in Fig. 2 along the tube axis for $Q=1$ l/min. As the gas temperature increases, the volumetric expansion of gas causes velocities to increase. The reverse of the above statement is true during cooling in the region ahead of the torch. In Fig. 2(a), which is the case without thermal radiation ($\kappa_o=0$), the axial velocity profile for the upward flow case (solid lines) accelerates from the entrance to the region near the torch ($x \approx 20$) over the entire cross section. In the near wall region ahead of the torch ($x>22$, $r>0.8$), the axial gas velocity accelerates, and thus the backward flow takes place in the central core region due to mass continuity. As the radiative absorption coefficient increases, in Fig.

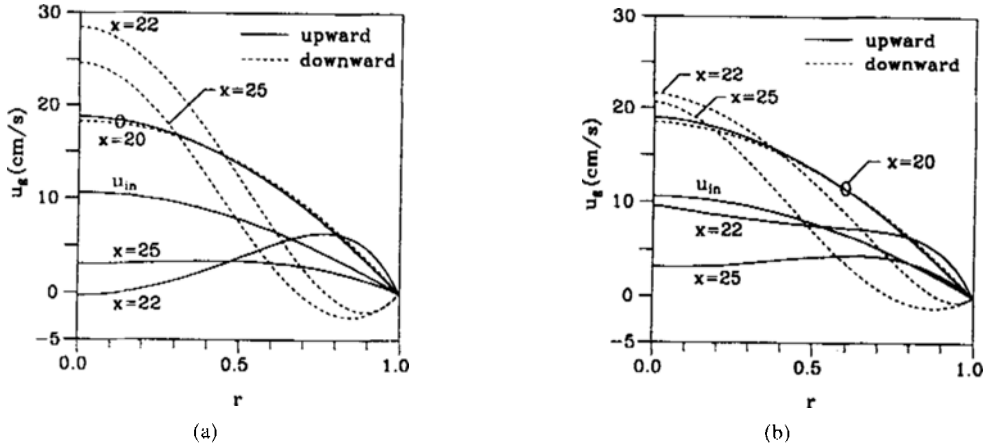

Fig. 2 Axial velocity distribution along the axial locations; Q=1 l/min., upward flow (solid lines), downward flow (dashed lines); (a) $\kappa_o=0\text{cm}^{-1}$, (b) $\kappa_o=0.5\,\text{cm}^{-1}$

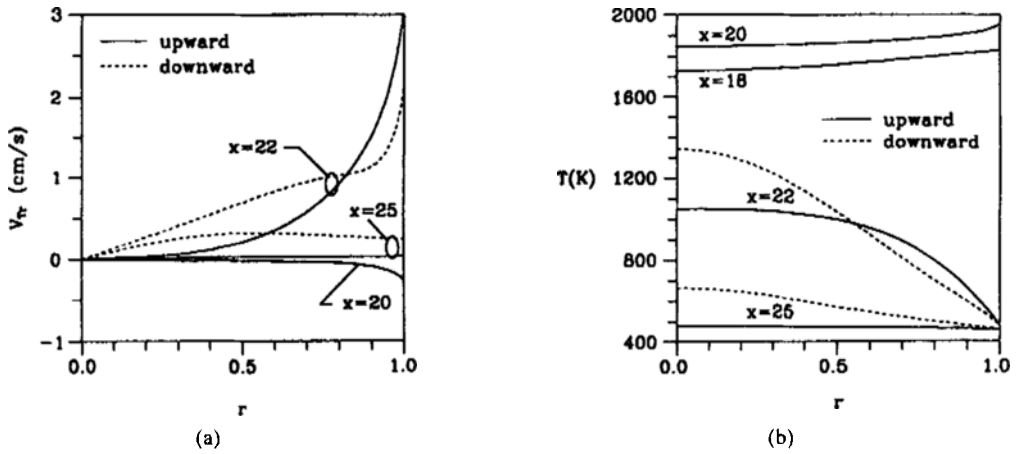

Fig. 3 The thermophoretic velocity (a) and temperature (b) distribution of radial component along the axial locations; $\kappa_o=0\,cm^{-1}$, Q=1 l/min., upward flow (solid lines), downward flow (dashed lines)

2(b), the backward flow in the central core region disappears because of the far reaching nature of the radiative heat transfer. For the downward flow case (dashed lines), the recirculation is formed in the near wall region ahead of the torch ($x \geq 22$) because of negative direction of buoyancy force, and thus the velocity in the central core region is more accelerated in order to satisfy the flow continuity. When the effect of radiative heat transfer is considered, the recirculation flow disappears in the near wall region of the ahead of the torch. Here, the variation of the radiative absorption coefficient can be achieved by using another kind of carrier gas (CO_2, He and O_2 etc.) or various amount of mass fraction of CO_2 in the carrier gas (Kim and Pratsinis, 1989).

The radial components of the thermophoretic velocity, for the case of neglecting thermal radiation effect and Q=1 l/min., are represented in Fig. 3 (a). For the case of upward flow (solid lines), the thermophoretic velocity has a negative sign (i. e. particles move toward the central region of the tube) in the region behind torch ($x \leq 20$), and a positive sign (i. e. particles move toward the tube wall) in the region ahead of the torch. The thermophoretic velocity decreases suddenly in the region ahead of the deposition zone ($x \geq 22$) as particles move downstream. This enables the deposition zone to exist. The thermophoretic velocity of downward flow (dashed lines) is almost same as that of upward flow in the region of $x \leq 20$, because the temperature profile of upward flow is very close to that of downward flow (Fig. 3 b). However, in the region ahead of the torch ($x \geq 22$), the thermophoretic velocity of downward flow is much larger than that of upward flow in the central region, and the reverse applies in the near wall region. This behavior can be explained by the following reasons. In the region behind the torch ($x \leq 20$), the gas temperature is lower than the wall temperature. The heated gas flows ahead of torch and thus may be higher temperature than the surrounding cold wall surface. Thus in the region ahead of the torch ($x > 20$), the wall temperature decreases rapidly to 453K. For the case of downward flow, the heated carrier gas in the central region is accelerated in the region ahead of the torch ($x \geq 20$) as can be seen in Fig. 2(a), higher temperature gradients would be expected.

As the radiative absorption coefficient increases (Fig. 4), the difference of thermophoretic velocities decreases between the upward and downward flow case. Figure 5 shows the distributions of radial particle velocity along the tube axis for the cases of with or without the thermal radiation. For the upward flow case, radial particle velocities at various axial locations are different from the radial component of thermophoretic velocities (Fig. 3 a). This phenomenon is due to the following reasons. The axial component of gas velocity represents a great difference because

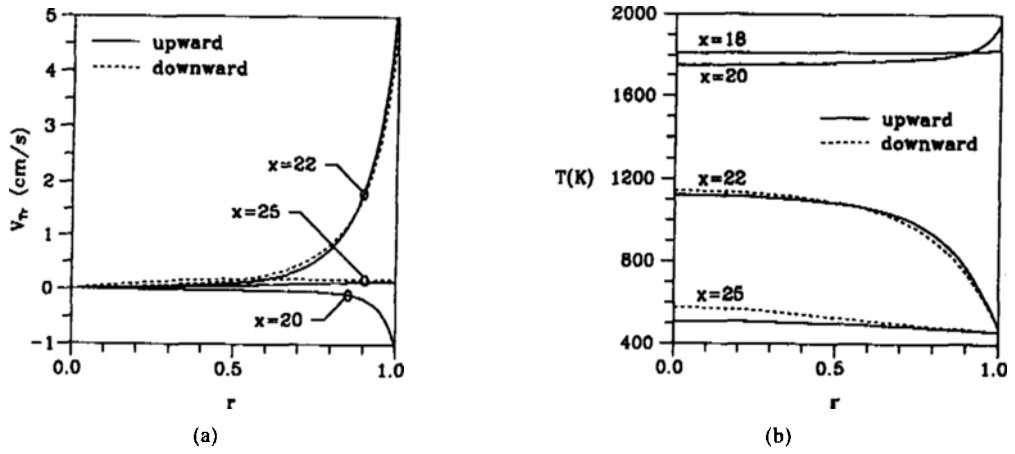

(a) (b)

Fig. 4 The thermophoretic velocity (a) and temperature (b) distribution of radial component along the axial locations; κ_o=0.5 cm^{-1}, Q=1 l/min., upward flow (solid lines), downward flow (dashed lines)

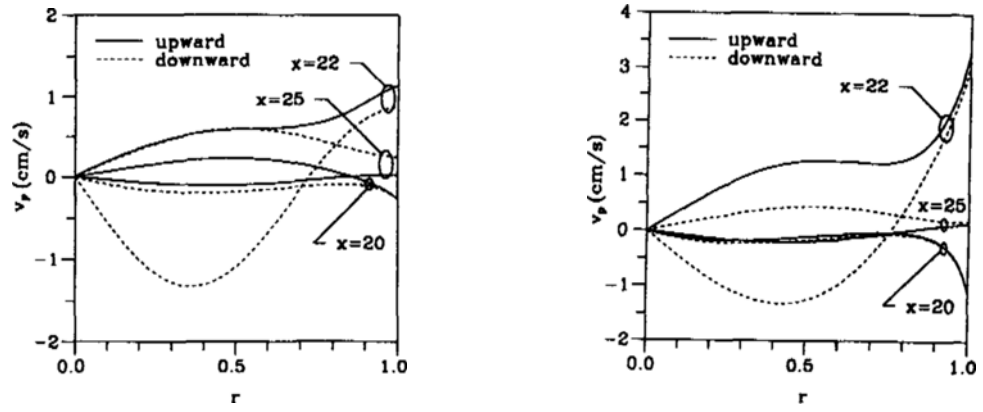

(a) (b)

Fig. 5 The particle velocity distribution of radial component along the axial locations; Q=1 l/min., upward flow (solid lines), downward flow (dashed lines) ; (a) κ_o= 0 cm^{-1}, (b) κ_o=0.5 cm^{-1}

of the gas volume expansion and buoyancy force shown in Fig. 2 (a). Thus the radial gas velocities represent a great difference. For the upward case, the axial gas velocity in the central region of the deposition zone ($r<0.5$, $x\approx22$) is accelerated due to the buoyancy force (Fig. 2 a), accordingly the radial gas velocity in this region is the negative sign, that is, the particles in this region move toward the tube center. Therefore, the radial particle velocity in the deposition zone ($x\approx22$) has the negative sign in the central region ($r<0.7$) where the thermophoretic velocity has the positive sign, that is, the particles in this region move toward the tube center. As the radiative absorption coefficient increases, in Fig. 5 (b), the radial particle velocities increase in the near wall region of the deposition zone ($x=22$, $r>0.9$).

Figure 6 (a) and (b) show particle trajectories for different flow rates of the carrier gas (Q=1 and 3 l/min.) without thermal radiation. Particles have been initiated at the same locations for the upward and downward flow condition. As the cool gas enters the hot zone (around the torch), it begins to be heated. At some point, where the carrier gas temperature is higher than the effective reaction temperature, particles form. As the gas and the particle keep flowing through the hot zone, the gas is heated further because the wall temperatures in the hot zone are higher than the effective reaction temperature. For both the up-

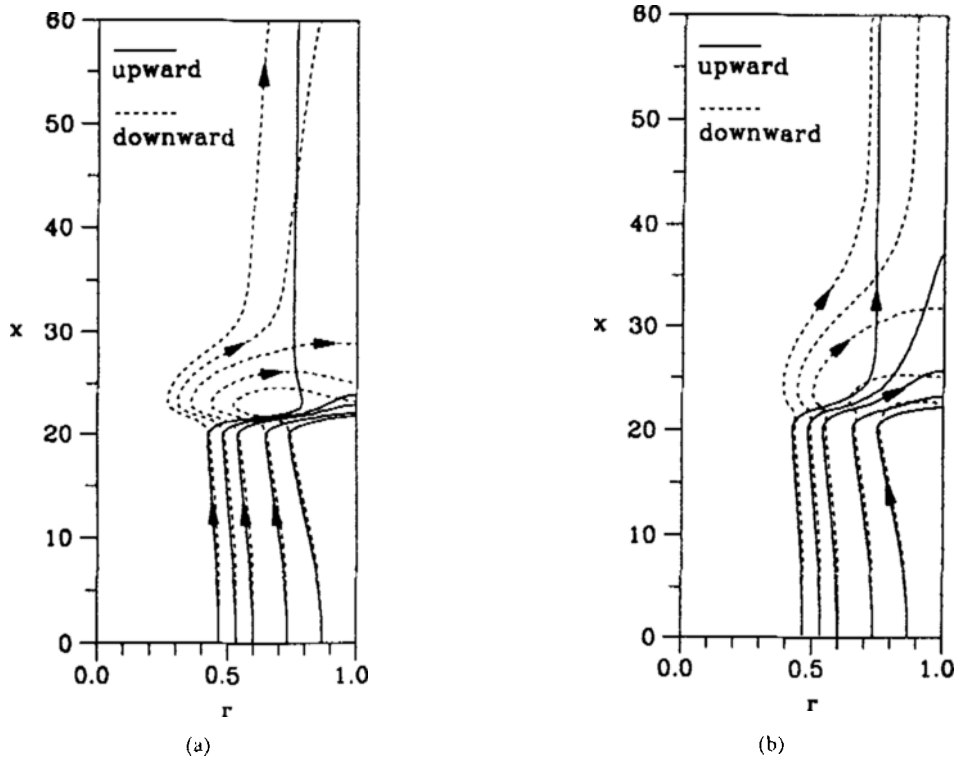

Fig. 6 Particle trajectories with $\kappa_o=0\,cm^{-1}$; upward flow (solid lines), downward flow (dashed lines); (a) Q=1 l/min., (b) Q=3 l/min.

ward flow and downward flow case, the particle moves toward the center of tube because the thermophoretic velocity has a negative sign in this region. For the upward flow case, in the farther downstream where the thermophoretic velocity (or particle velocity) has positive signs, the particle reverses direction and starts moving toward the wall. This causes particle deposition in a finite zone ahead of the torch (deposition zone). However, for the downward flow case, the particle moves suddenly toward the center of the tube in the region ahead of the torch (x>20), and then in the farther downstream the particle reverses the direction and starts moving toward the tube wall. This behavior is due to the following reason. The radial gas velocity moves toward the center of the tube because the axial gas velocity is accelerated in the central region. Thus the radial particle velocity moves toward the center of the tube (Fig. 5). Farther downstream (about x=25), the particle velocity has the positive sign, i. e., particles reverse the direction and start moving toward the tube wall. Therefore the deposition zone of the downward flow is broader than that of the upward flow. When the flow rate of carrier gas is 3 l/min., the extent that particle trajectories excute a turn becomes weaker, and deposition zone is broader than the case of Q=1 l/min. When the radiative heat transfer is considered (Fig. 7), unlike the case that the thermal radiation is neglected (Fig. 6), the particle moves parallel to the tube axis in the region behind torch (x<20). The deposited particles are those which start moving (are formed) in the vicinity of the tube wall, but the particles issuing (are formed) near the center of the tube are carried out the exhaust.

Figure 8 shows the deposition efficiency along the tube axis for different radiative absorption coefficients and flow rates. Here the variation of the radiative absorption coefficient can be achieved by using the other absorption coefficient of carrier gas (O_2, He, CO_2) or the magnitude of the formed particle number concentration. When radiation effect is neglected ($\chi_o=0$, solid line),

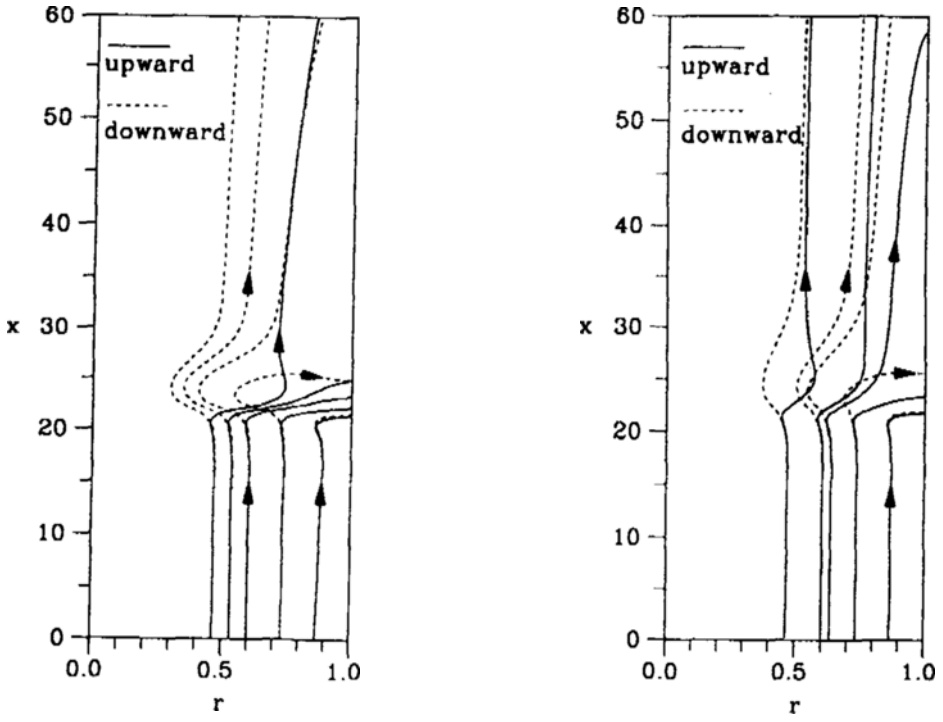

Fig. 7 Particle trajectories with $\kappa_o=0.5\,cm^{-1}$; upward flow (solid lines), downward flow (dashed lines); (a) Q=1 l/min., (b) Q=3 l/min.

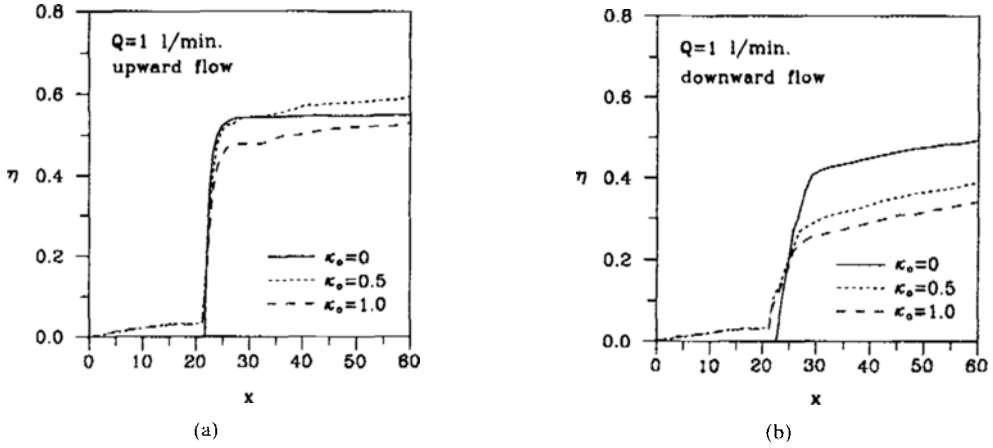

Fig. 8 Particle deposition efficiencies as a function of absorption coefficient with Q=1 l/min.; (a) upward flow, (b) downward flow

most of particle deposition is accomplished in the deposition zone ($x\approx22$). When the thermal radiative heat transfer exists, the carrier gas flowing in the region behind the torch ($x<20$) heats by virtue of thermal radiation, and thus a small value of thermophoretic velocity exists near the wall in this region. Therefore a slight amount of particles issued into the tube close by the wall is deposited on the tube wall. For the downward flow case, the deposition zone is broader than the case of the upward flow, and the particle deposition is accomplished a little in the downstream.

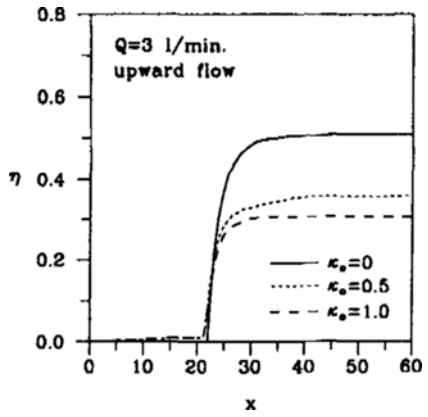

(a)

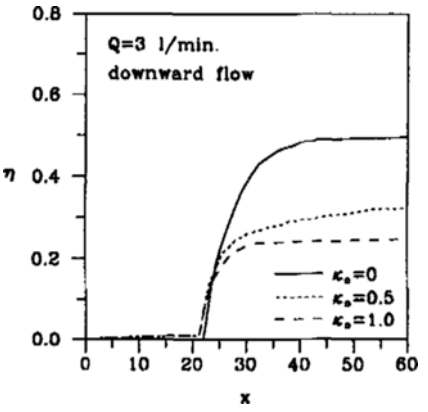

(b)

Fig. 9 Particle deposition efficiencies as a function of absorption coefficient with Q=3 l/min.; (a) upward flow, (b) downward flow

This behavior makes the non-uniform deposition of axial direction even if the torch moves cyclically along the tube axis. As the carrier gas flow rates increase(Fig. 9), the deposited efficiencies become low, the deposition zone comes to be broad, and the differences of efficiency between κ_o =0 case and κ_o=0.5, 1.0 case increase.

4. Conclusions

A particulate two phase flow with non-uniform wall temperature has been studied for the deposition of particles including the effects of the thermal radiation and mixed convection with application to the manufacture of optical fiber preforms. The present study focuses on predicting the particle transport characteristics and deposition efficiency/rate in the vertical tube flow with variable wall temperature because of the ring torch. The following conclusions are made.

(1) As the carrier gas flow rate increases, the deposition zone becomes broader and particle deposition efficiency decreases.

(2) When thermal radiative heat transfer exists, a slight amount of particles issued into the tube close by the wall is deposited on the tube wall in the region behind the torch(x<20), and the deposition zone becomes broader. Thus these behaviors make the non-uniform particle deposition in the axial direction.

(3) The particle deposition efficiency/rate in the upward flow case is more enhanced than that in the downward flow case. The deposition zone is broader for the downward flow than that for the upward flow case.

Reference

Cho, J. and Choi, M., 1995, "An Experimental Study of Heat Transfer and Particle Deposition for the Modified Chemical Vapor Deposition," *J. of Heat Transfer*, Vol. 117, pp. 1036~1041.

Cho, J. and Choi, M., 1994, "An Experimental Study of the Modified Chemical Vapor Deposition Process-Temperature Distribution and Particle Deposition Measurements," *Trans. of KSME*, Vol. 18, pp. 3057~3065.

Choi, M., 1992, "Chemical Vapor Deposition Technology in the Optical Fiber Preform Manufacturing Process(in Korean)," *J. of KSME*, Vol. 32, No. 8, pp. 673~684.

Crowe, C. T., 1982, "Review - Numerical Models for Dilute Gas-particle Flows," *J. of Fluid Eng.*, Vol. 104, pp. 297~303.

Fuchs, N. A., 1964, *The Mechanics of Aerosols*, Pergamon Press, New York .

Jia, G., Yener, Y. and Cipolla, J. W., 1992, "Thermophoresis of a Radiating Aerosol in Thermally Developing Poiseuille Flow," *Int. J. Heat and Mass Transfer*, Vol. 35, pp. 3265~3273.

Kim, K. S. and Pratsinis, S. E., 1989, "Modeling and Analysis of Modified Chemical Vapor Deposition of Optical Fiber Preforms," *Chemical*

Eng. Sci., Vol. 44, pp. 2475~2482.

Kim, Y. J. and Kim, S. S., 1991, "Particle Size Effects on the Particle Deposition from Non-isothermal Stagnation Point Flows," *J. Aerosol Sci.*, Vol. 22, pp. 201~214.

Kim, Y. J. and Kim, S. S., 1992, "Experimental Study of Particle Deposition onto a Circular Cylinder in High-temperature Particle-laden Flows," *Experimental Thermal and Fluid Sci.*, Vol. 5, pp. 116~123.

Lin, Y. T., Choi, M. and Grief, R., 1992, "A Three-Dimensional Analysis of Particle Deposition for the Modified Chemical Vapor Deposition (MCVD) Process," *J. of Heat Transfer*, Vol. 114, pp. 735~742.

Menguc, M. P. and Viskanta, R., 1986, "Radiative Transfer in Axisymmetric, Finite Cylindrical Enclosures," *J. of Heat Transfer*, Vol. 108, pp. 271~276.

Moore, M. J. and Crane, R. I., 1973, "*Deposition and Corrosion in Gas Turbine*," Edited by Hart, A. B. and Cutler, A. J. B. Chap. 4, John Wiley and Sons, New York.

Nagel, S. R., MacChesney, J. B. and Walker, K. L., 1982, "An Overview of the Modified Chemical Vapor Deposition (MCVD) Process and Performance," *IEEE J. of Quantum Electronics*, QE-18, 459~476.

Park, K. S. and Choi, M., 1994, "Conjugate Heat Transfer and Particle Deposition in the Modified Chemical Vapor Deposition Process: Effect of Torch Speed and Solid Layer," *Int' J. Heat and Mass Transfer*, Vol. 37, pp. 1593~1603.

Park, S. H. and Kim, S. S., 1993, "Thermophoretic Deposition of Absorbing, Emitting and Isotropically Scattering Particles in Laminar Tube Flow with High Particle Mass Loading," *Int. J. Heat and Mass Transfer*, Vol. 36, pp. 3477~3485.

Patankar, S. V., 1980, "*umerical Heat Transfer and Fluid Flow*, McGraw-Hill, New York.

Pratsinis, S. E. and Kim, K. S., 1989, "Particle Coagulation, Diffusion and Thermophoresis in Laminar Tube Flow," *J. Aerosol Sci.*, Vol. 20, pp. 101~111.

Rosner, D. E. and Kim, S. S., 1984, "Optical Experiments on the Thermophoretically Augumented Submicron Particle Deposition from Dusty High Temperature Gas Flows," *Chemical Eng'g* J., Vol. 29, pp. 147~157.

Rosner, D. E. and Park, H. M., 1988, "Thermophoretically Augumented Mass, Momentum and Energy Transfer Rates in High Particle Mass Loaded Laminar Forced Convection Systems," *Chemical Eng'g Sci.*, Vol. 43, pp. 2689-2704.

Talbot, L., Cheng, R. K., Schefer, R. W. and Willis, D. R., 1980, "Thermophoresis of Particles in a Heated Boundary Layers," *J. Fluid Mech.*, Vol. 101, pp. 737~758.

Walker, K. L., Geyling, F. T. and Nagel, S. R., 1980, "Thermophoretic Deposition of Small Particles in the Modified Chemical Deposition (MCVD) Process," *J. of the American Ceramic Society*, Vol. 63, pp. 552~558.

Yoa, S. J., Kim, S. S. and Lee, J. S., 1990, "Thermophoresis of Highly Absorbing, Emitting Particles in Laminar Tube Flow," *Int. J. Heat and Fluid Flow*, Vol. 11, pp. 98~104.

Zeldin, B. and Schmidt, F, W., 1972, "Developing Flow with Combined Forced-Free Convection in an Isothermal Vertical Tube," *J. of Heat Transfer*, Vol. 94, pp. 211~223.